Probing the Nucleotide Binding Sites of Axonemal Dynein with the Fluorescent Nucleotide Analogue 2′(3′)-*O*-(-*N*-Methylanthraniloyl)-adenosine 5′-Triphosphate[†]

Gabor Mocz,*,[‡] Michael K. Helms,[§] David M. Jameson,[§] and I. R. Gibbons[‡,||]

Pacific Biomedical Research Center, University of Hawaii at Manoa, 1993 East-West Road, Honolulu, Hawaii 96822, and Department of Genetics and Molecular Biology, University of Hawaii at Manoa, 1960 East-West Road, Honolulu, Hawaii 96822

ABSTRACT: MantATP [2′(3′)-*O*-(-*N*-methylanthraniloyl)-adenosine 5′-triphosphate] was employed as a fluorescence probe of the nucleotide-binding sites of dynein from sea urchin sperm flagella. MantATP binds specifically with enhanced fluorescence (∼2.2-fold), homogeneous lifetime (8.4 ns), and high anisotropy ($r \sim 0.38$) to dynein and can be displaced by ATP and ADP added to the medium. The association constants of mantATP complexed with dynein were determined from anisotropy titration data. Using a multiple stepwise equilibrium model, the average values of the first two association constants are $K_1 = 2.7 \times 10^5$ M^{-1} and $K_2 = 1.8 \times 10^4$ M^{-1}. This value of K_1 is 7−8 times higher than that found previously for unsubstituted ATP, whereas K_2 is little changed [Mocz and Gibbons (1996) *Biochemistry 35*, 9204−9211]. The lower-affinity binding sites, K_3 and K_4, observed previously could not be studied with mantATP within the available protein concentrations. The α and β heavy chain subfractions have binding parameters similar to those of intact dynein. Formation of the stable ternary complex of mantATP with dynein and monomeric vanadate is accompanied by only a moderate increase in the binding affinities. Oligomeric vanadate reduces the binding affinities by ∼50%. Addition of TritonX-100, methanol, or various salts changes the binding affinities by up to 50%, suggesting that the microenvironment of the nucleotide-binding sites involves significant contributions from both polar and apolar interactions. The distinct affinities of the individual binding sites are consistent with a physiological role in regulating nucleotide binding.

Dynein ATPases form a widely distributed class of motor proteins that transduce the free energy of ATP hydrolysis into mechanical work. They are involved in many diverse forms of microtubule-based cell motility, including ciliary and flagellar movement (*1−3*), organelle and vesicle transport toward the minus end of cytoplasmic microtubules (*4, 5*), and normal nuclear segregation in yeast (*6*), as well as a wide variety of other essential cellular movements (*7−11*).

Most of the known functional aspects of dynein are currently attributed to its heavy chain polypeptide subunits (M_r > 500 000). These include ATP-sensitive tubulin binding and the binding and hydrolysis of nucleotide. Dynein is believed to contain multiple, functionally distinct binding sites for adenine nucleotides, only one of which participates directly in hydrolysis. The amino acid sequences of the heavy chains in both axonemal (*12−15*) and cytoplasmic dyneins (*16, 17*) contain four copies of the sequence motif

for a nucleotide-binding site (P-loop, (*18*)), spaced about 300 residues apart in the midregion of the chain. The P-loop corresponding to the hydrolytic ATP-binding site can be identified by its location close to or at the V1 site of vanadate-mediated photocleavage (*19*). The region around this hydrolytic site, P1, has the most highly conserved sequence among dynein isoforms (*20*). The less tightly conserved P-loops, P2−P4, may constitute parts of regulatory nucleotide-binding sites. Consistent with this hypothesis, equilibrium partition analysis has indicated that dynein heavy chains from sea urchin sperm flagella may contain four different binding sites for nucleotide triphosphates per mole of heavy chain (*21*). The stepwise association constants for ATP range from 10^4 to 10^5 M^{-1}, consistent with nucleotide binding to putative regulatory sites occurring at physiological concentrations. More direct evidence of regulatory function is provided by reports that the axonemal motility in vitro is inhibited by high concentrations of ATP, with the inhibition being reversible by addition of ADP (*22−24*). Kinetic analysis of the dynein ATPase at low (micromolar) ATP concentrations shows simple Michaelis−Menten kinetics with a K_M of ∼1 μM (*25*), whereas analysis at higher concentrations shows nonlinear kinetics with two K_M's of 8−11 and 66−80 μM, respectively (*23*).

A useful way to study the properties of nucleotide-binding sites on an enzyme is provided by the changes in fluorescence of the ATP analogue, mantATP,[1] that occur upon its binding

to the enzyme (*26*). For many ATPases the steady-state parameters of binding and hydrolysis of mantATP are close to those of unmodified ATP, possibly because the attachment of the fluorescent reporter group predominantly to the 3′ position on the ribose allows unobstructed interaction of the adenine base with the binding site on the protein (*27, 28*). Both mantATP and the related fluorescent derivative anthraniloyl-ATP are efficient substrates for dynein ATPase and support flagellar motility (*29−31*).

In this work, we use mantATP to study the properties of the ATP-binding sites of soluble dynein from sea urchin sperm flagella. By determining the increase in fluorescence anisotropy of mantATP upon binding, we will obtain the equilibrium profile for the binding of this nucleotide to dynein in physiological medium. The number and affinities of binding sites will be estimated and related to the physiological function of dynein. Effects of a series of salts and organic solvents on the binding affinities will also be observed.

EXPERIMENTAL PROCEDURES

Chemicals. MantATP was a generous gift from Dr. John F. Eccleston (NIMR, Mill Hill, London, U.K.). Adenine nucleotides (ATP, ADP) came from Boehringer Mannheim (Germany). Dimethyl-POPOP was purchased from Molecular Probes (Eugene, OR). All other chemicals were analytical grade from Sigma (St. Louis, MO).

Protein Preparations. Outer arm dynein with latent ATPase activity was extracted from sperm of the sea urchin *Tripneustes gratilla* as previously described (*32*). The dynein was then transferred to 0.5 M acetate-based medium by dialysis and purified to remove tubulin by centrifugation on sucrose gradients. The separated α and β heavy chain fractions were obtained by dialysis of the dynein against 1 mM EDTA and 25 mM Tris/SO$_4$, pH 7.4, medium, followed by centrifugation on 5−20% sucrose gradients (*32*). All samples were concentrated by precipitation with 60% saturated $(NH_4)_2SO_4$. In preparation for use, the protein was resuspended and exchanged into a standard low ionic strength buffer containing 2 mM MgSO$_4$ and 25 mM Tris/SO$_4$, pH 7.4, and then dialyzed into the same medium before beginning fluorescence experiments.

Generation of Fluorescence Anisotropy Binding Isotherms. Fluorescence anisotropy measurements were carried out on an ISS model K2 fluorometer (Champaign, IL), using a xenon arc lamp as the light source. Excitation was at 360 nm, and emission was observed through a Schott KV-399 cuton filter, which passes light above 380 nm. All measurements were done at room temperature (∼23 °C). Fluorescence titrations of mantATP with dynein were performed in a 0.4 × 1.0 cm cuvette (path length was 1.0 cm, initial volume 0.6 mL) by adding aliquots of protein stock solutions, with subsequent mixing, to a fixed initial concentration of the fluorescent nucleotide. Samples were in standard low ionic strength buffer. Other salts or organic solvents were sometimes added as required for particular experiments. Contributions to the fluorescence intensity from the buffer and protein (e.g., scattering) were subtracted. The average

standard deviation of anisotropy in all samples was 0.002 or less (an average of 5−7 readings per measurement).

The ratio of the lifetime of bound mantATP to that of free mantATP was taken as the enhancement factor, or enhancement of the quantum yield upon binding, and used in calculating concentrations of free and bound mantATP, and ultimately in calculating association constants. The fluorescence lifetimes of mantATP free in solution and bound to dynein were measured on the same ISS model K2 instrument by using the frequency domain approach (*33, 34*). Excitation was at 363.8 nm using a Spectra-Physics Model 2045 argon ion laser as a light source. Emission was observed through a Schott KV-399 cuton filter. Lifetimes were analyzed using the Globals Unlimited software (Laboratory for Fluorescence Dynamics, University of Illinois, Urbana-Champaign). A computational model containing discrete components for the lifetimes of bound and free mantATP was used. The lifetime of free mantATP was linked between data sets, but the bound lifetime and fractions of each were allowed to vary.

Data Analysis: Multiple Stepwise Binding Model. On formation of mantATP/dynein complexes, the total fluorescence emission intensity (*F*) and anisotropy (*r*) are given by

$$F = \sum c_i F_i \tag{1}$$

$$r = \sum c_i F_i r_i / F \tag{2}$$

where c_i is the concentration of species i, F_i is its fluorescence emission intensity per unit concentration, and r_i is its anisotropy. Using the additivity of the anisotropy function [(*35*), which followed directly from the original relations of the additivity of polarization derived by Weber (*36*)], the fraction of mantATP bound to dynein, *x*, is determined from these equations by

$$x = (r - r_f)/(r_b - r_f + (g - 1)(r_b - r)) \tag{3}$$

where r_f is the anisotropy of mantATP free in solution, r_b is the anisotropy of the bound nucleotide, that is, the limiting anisotropy, *r* is the observed anisotropy, and *g* is the enhancement factor. The same enhancement factor is assumed for all sites as it would be impossible to determine each separately.

This equation can be rewritten in terms of the binding parameters as

$$x = n\Theta S_t / L_t \tag{4}$$

where *n* is the number of binding sites, Θ is the fraction of *sites* to which mantATP is bound, that is, saturation, S_t is the total protein, and L_t is the total nucleotide concentration, respectively.

In terms of the association constants, the quantity $n\Theta$ for a heavy chain of dynein capable of binding multiple nucleotide molecules can be expressed by the multiple stepwise equilibrium model as

$$n\Theta = \sum j[\text{mantATP}]^j \, \Pi \, K_j / (1 + \sum [\text{mantATP}]^j \, \Pi \, K_j) \tag{5}$$

where

---

[1] Abbreviation: mantATP, 2′(3′)-*O*-(-*N*-methylanthraniloyl)-adenosine 5′-triphosphate.

$$[\text{mantATP}] = (1 - x)L_\text{t} \qquad (6)$$

is the free nucleotide concentration, j ranges from 1 to the number of sites, and K_j is the jth association constant.

Nonlinear Curve Fitting. The association constants were calculated from eq 5 using an iterative nonlinear procedure based upon rigorous least-squares adjustments (*37*). In the initial fitting stage, equivalent binding sites were assumed and the initial input parameters (the rough association constants) were calculated as

$$K = \sum \Theta / \sum (1 - \Theta)[\text{mantATP}] \qquad (7)$$

and then, in the iterative procedure, the values of these parameters were adjusted to minimize the difference between the modeled and experimental data.

Application of eq 5 also involves the evaluation of the limiting anisotropy r_b as it appears indirectly via eq 3. Computationally determined asymptotic values of this quantity and estimates made by treating the limiting anisotropy as an adjustable parameter were both close to the anisotropy of mantATP recorded directly by exciting at 360 nm in 100% glycerol at 5 °C where the fluorophore is maximally polarized (data not shown). Therefore, for all final computations, the limiting anisotropy was fixed with good confidence at the experimental value of 0.384.

Once the association constants were recovered, the experimental binding profiles, that is, anisotropy r versus protein concentration S, were modeled and reconstructed as

$$r = r_\text{f} + gx(r_\text{b} - r_\text{f})/(x(g - 1) + 1) \qquad (8)$$

$$S = (L_\text{o}S_\text{o} - [\text{mantATP}])/(n\Theta S_\text{o} + [\text{mantATP}]) \qquad (9)$$

where S_o is the initial dynein and L_o is the initial mantATP concentration, respectively.

Nucleotide Concentrations. The concentrations of nucleotides were determined using $\epsilon = 5800 \ \text{M}^{-1} \ \text{cm}^{-1}$ at 356 nm for mantATP (*26*) and $\epsilon = 15\ 400 \ \text{M}^{-1} \ \text{cm}^{-1}$ at 259 nm for ATP and ADP (*38*).

Protein Concentrations. Protein concentrations were determined spectrophotometrically by an absolute method based upon the difference in absorbance at 235 and 280 nm (*39*). The molecular weights used were the following: dynein, 750 000/chain; α chain subfraction, 550 000/chain; β chain subfraction, 650 000/chain.

ATPase Activity. ATPase activities of stock solutions of dynein and its subfractions were measured at room temperature in the standard low ionic strength buffer. The inorganic phosphate liberated was determined by the method of LeBel (*40*).

RESULTS

Fluorescence Anisotropy and Lifetime Measurements. The fluorescence of mantATP free in solution is highly depolarized ($r = 0.025$), consistent with the rotation of a small molecule. Incremental additions of dynein to solutions of mantATP produce a 15−20-fold increase in anisotropy as well as a ∼2.2−2.3-fold increase in fluorescence intensity of the fluorophore.

The increase in quantum yield of mantATP upon binding to dynein was calculated by measuring the excited-state

Table 1: Fluorescence Enhancement of MantATP upon Binding to Dynein and Its Subfractions[a]

sample	enhancement factor
1 μM mantATP + 5 μM dynein	2.3
1 μM mantATP + 5 μM α chain	2.2
1 μM mantATP + 6 μM β chain	2.1

[a] Fluorescence lifetimes of free and bound mantATP were measured using multifrequency phase and modulation fluorometry. A model consisting of three discrete lifetime components best described the data, and values of the reduced χ^2 ranged from 1 to 3. The long component (∼8.5 ns) represents bound mantATP, the middle component (∼3.8 ns) represents free mantATP, and the short component (∼0.9 ns) is attributed to a combination of scattered light and a minor lifetime component of free mantATP. Enhancement factors show changes in lifetimes due to binding of the fluorescent nucleotide to dynein and its heavy chain subfractions.

lifetimes of bound and free mantATP. Free mantATP has a heterogeneous lifetime, with components of ∼3.8 and ∼0.9 ns. A single lifetime of ∼8.5 ns appears upon binding of mantATP to dynein, in addition to the two lifetimes of the free mantATP. The fractions of each lifetime then relate to the relative amounts of free and bound nucleotide.

The ratio of the lifetimes of bound and free mantATP, or enhancement factors, are reported in Table 1. The binding increases the lifetimes, and therefore the quantum yields, by ∼2.1−2.3-fold both with intact dynein and with its heavy chain subfractions. These values are consistent with the maximum fluorescence intensity changes observed upon binding. The relative amounts of free and bound nucleotide from the lifetime measurements gave association constants consistent with those reported from titration experiments below, but are somewhat less accurate because they represent only a single point titration and are therefore not shown.

Binding Isotherms. The fluorescence anisotropy of mantATP as a function of dynein concentration is plotted in Figure 1A together with the corresponding data fits (see below, Binding Parameters). These measurements were performed by adding successive aliquots of dynein to solutions of mantATP in standard assay buffer (also containing 100 mM K_2SO_4); therefore the final concentration of both nucleotide and protein was varied for each series of measurements. The extent of binding as a function of free mantATP concentration is shown in Figure 1B.

The fluorescence changes show saturation behavior; however, complete saturation is not attained because the concentration of the protein required for reaching saturating values of anisotropy was above the solubility limit of dynein. The anisotropy values reached equilibrium very quickly (within seconds) and remained constant over several minutes, which was the time course of these experiments, suggesting that mantATP (and its hydrolysis product, mantADP) remains bound to dynein (data not shown). The total change in anisotropy observed at maximum protein concentration was consistent between replicate experiments with a given dynein preparation but was somewhat less reproducible between preparations. A limiting anisotropy of 0.384 was used for all calculations as described in Experimental Procedures. This choice of limiting anisotropy is a more reasonable assumption than treating the limiting anisotropy as an adjustable parameter in the fitting of data. The coincidence of the extrapolated value near 0.38 with the limiting value of
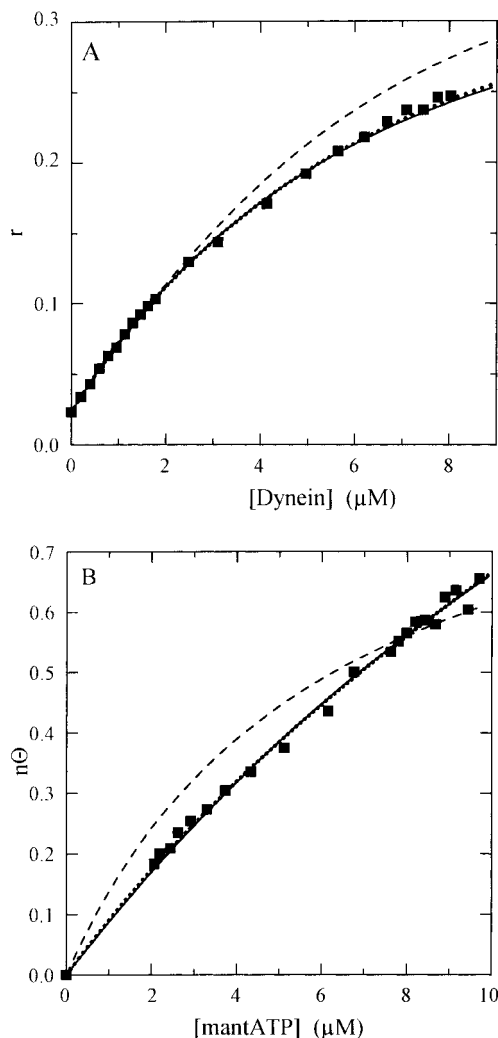
FIGURE 1: Binding of mantATP to intact dynein (M_r = 750 000/chain) as measured by fluorescence anisotropy. (A) Equilibrium titration with dynein: anisotropy (r) versus total protein concentration. The initial concentration of mantATP was 10 μM in 20 mM Tris/SO$_4$, 100 mM K$_2$SO$_4$, and 2 mM MgSO$_4$, pH 7.4. The titration was carried out at room temperature. (B) Plot of the equilibrium titration data as a binding curve: binding function (extent of binding, $n\theta$) versus free nucleotide concentration. The binding function is defined by eq 5 under Experimental Procedures. The points in the figure are experimental. The lines in Panel B represent fitting of the data with the binding parameters obtained using a nonlinear least-squares routine over eq 5. As a measure of goodness of fit, the mean deviation (σ) is computed as the mean squared difference between the observed values and the corresponding values calculated from the final parameter values. Dashed line (---): only one site is assumed in the binding model (σ = 0.01078). Solid line (—): two sites are assumed (σ = 0.00286). Dotted line (···): three sites are assumed (σ = 0.00273). The lines on Panel A represent the reconstructed titration curves (eq 8−9) using the estimated best-fit binding parameters. The binding parameters for the first two sites are summarized in Table 2 along with the measured enhancement factors, Table 1. The data show a single representative experiment. Separate experiments with independent protein preparations gave similar results within experimental error.

immobilized mantATP suggests that the bound fluorophore does not undergo significant local motion.

Figures 2 and 3 show isotherms for binding of mantATP to the α and β heavy chain subfractions, respectively. As with dynein, a negatively curved titration response showing saturating behavior was observed. Each of the separated
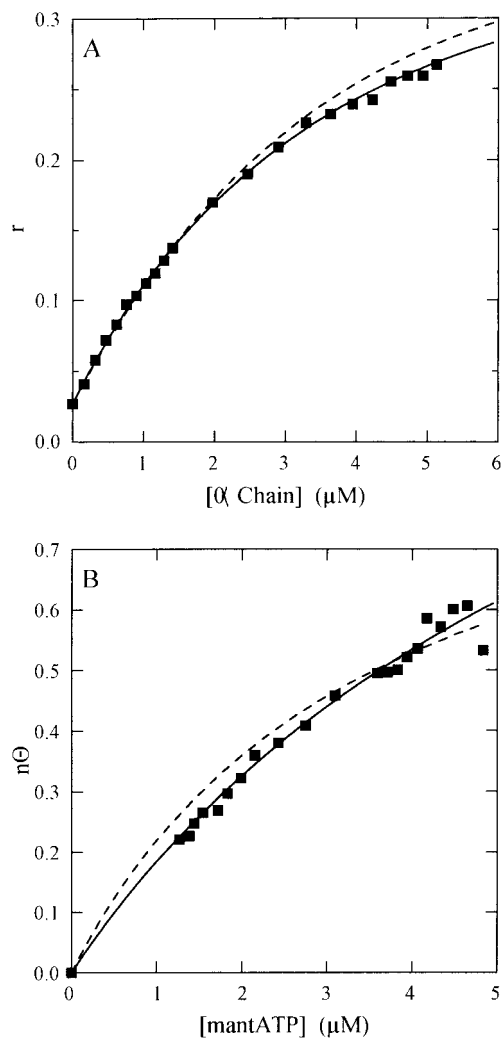

FIGURE 2: Effect of increasing concentrations of α heavy chain subunit of dynein (M_r = 550 000/chain) on the fluorescence anisotropy of mantATP. (A) Anisotropy (r) as a function of total protein concentration. (B) Binding function ($n\theta$) versus free nucleotide concentration. The initial concentration of mantATP was 5 μM. Conditions otherwise were the same as with dynein in Figure 1. Dashed line (---): one site is assumed (σ = 0.00741). Solid line (—): two sites are assumed (σ = 0.00450).

heavy chain subfractions appears to bind mantATP to essentially the same extent as intact dynein.

The binding of mantATP to dynein and its subfractions can be reversed by addition of millimolar concentrations of ATP or ADP. This reversibility suggests that ATP, ADP, and mantATP compete for the same binding site(s). AMP failed to reverse the binding of mantATP (data not shown).

Binding Parameters. The parameters that describe the equilibrium binding of mantATP to dynein are the association constants K_i and the nucleotide/protein stoichiometry n, determined by the anisotropy titrations. Application of the stepwise binding model involves the evaluation of only n parameters. In this model, the nth nucleotide binds with a different association constant than the previous one. The majority of our data, that is, binding isotherms obtained in a range of [dynein] from 0 to 8 μM and [mantATP] either 1, 2, 5, or 10 μM can be adequately explained by a minimum of two sites per chain. Adding a third or fourth site to the binding model only marginally improves the curve fittings of the available data (dotted line, Figure 1). As a conse-
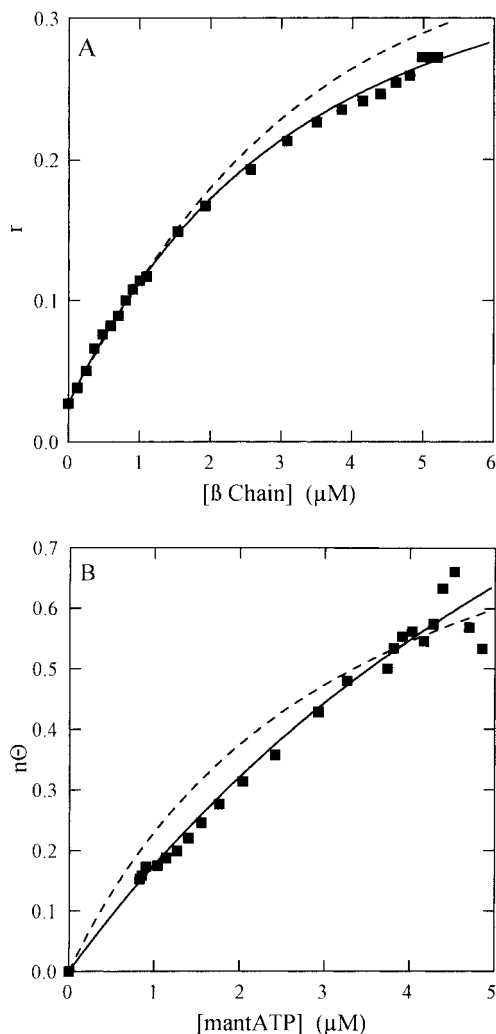
FIGURE 3: (A and B) Interaction of mantATP with the β heavy chain subunit of dynein ($M_r = 650\,000$/chain). The initial concentration of mantATP was 5 μM. The experimental conditions and abbreviations were as in Figure 1. Dashed line (---): one site is assumed ($\sigma = 0.0108$). Solid line (—): two sites are assumed ($\sigma = 0.0061$).

Table 2: Stepwise Association Constants for Binding of MantATP to Dynein and Its Heavy Chain Subunits[a]

sample	K_1	K_2
MantATP Binding to Dynein Determined from Fluorescence Anisotropy[b]		
dynein	26.9 ± 2.9	1.8 ± 0.5
α chain	24.4 ± 3.0	3.7 ± 2.2
β chain	21.6 ± 0.2	6.4 ± 2.2
ATP Binding to Dynein Obtained Previously from Phase Partition Analysis[c]		
dynein	3.3 ± 0.4	2.0 ± 0.2
α chain	0.8 ± 0.1	1.5 ± 0.2
β chain	2.8 ± 0.4	3.0 ± 0.6

[a] All values are given in units of $10^4 \times \mathrm{M}^{-1}$. Only the first two constants, K_1 and K_2, are considered. [a] Binding constants were determined using multiple stepwise equilibrium analysis applied to anisotropy data. [b] Values for ATP binding obtained from phase partition analysis are also shown for comparison (*21*). Uncertainties shown are standard errors. Data are obtained from at least 5 individual datasets in each case.
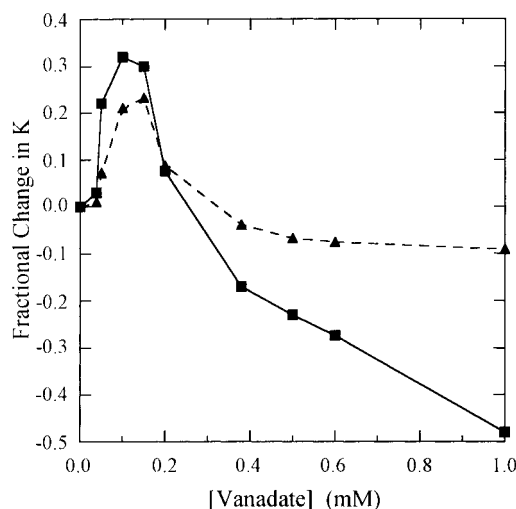

FIGURE 4: Fractional change in binding constants K_1 and K_2 as a function of vanadate concentration. The binding constants were determined from the individual isotherms at each vanadate concentration. The fractional change in K_i is given by $(K_v - K_i)/K_i$ where K_v is the constant observed at a given vanadate concentration. K_i is the constant in the absence of vanadate. Solid line (—): K_1 Dashed line (---): K_2.

quence, the quantitative determination of the binding affinities at these weak sites is not possible and the available data are insufficient to distinguish between models with 2 or with more than 2 sites. Impractically high concentrations of protein would be needed in the anisotropy titrations to describe the weak sites with confidence. Therefore, only the first two sites will be considered in detail.

The obtained association constants for the first two sites are summarized in Table 2. The association constant at the first site is 7—8-fold higher than that of the unsubstituted parent nucleotide measured previously by equilibrium partition (*21*). The affinities obtained for the second site appear comparable in both methods with only a slightly higher affinity for the fluorescent derivative.

Binding in the Presence of Vanadate. To characterize the interaction of mantATP with dynein more fully, we studied the effect of vanadate on the apparent binding affinities of mantATP by performing a series of anisotropy titrations in the presence of vanadate. At low micromolar concentrations, vanadate acts as a phosphate analogue, and has been shown to be an inhibitor of dynein ATPase by forming a dead-end kinetic block (*41, 42*). At submillimolar concentrations,

vanadate exists in oligomeric forms, and is an analogue of the polyphosphate chain of ATP. As seen in Figure 4, in the presence of monomeric vanadate (<0.2 mM), a ~40% increase in binding affinity at the first site was apparent. Oligomeric vanadate (>0.2 mM) appeared to reverse this effect and decreased the affinity to 60% of the initial value. The effect of vanadate on the affinity at the second site was similar, although somewhat smaller in extent. These results suggest structural differences in dynein when various forms of vanadate are interacting with or incorporated in the dynein/mantATP complexes. The changes could represent local perturbation of the microenvironment around the nucleotide-binding site.

Effect of Apolar Factors. The nature of the interaction of the *N*-methylanthraniloyl moiety of mantATP with the protein has been probed by determining the effect on the binding affinity of adding an apolar solvent to the medium. To take into account the effect of added solvent on quantum yield
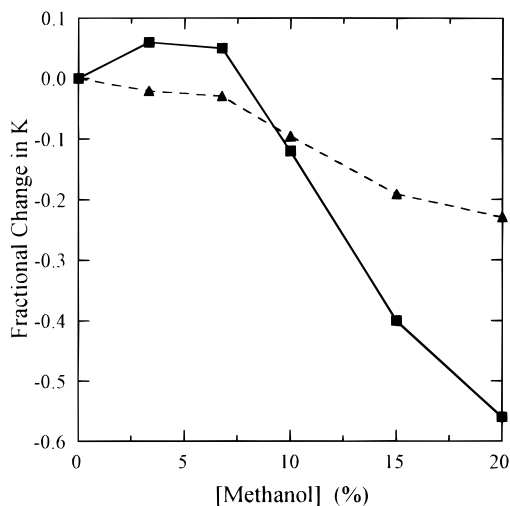
FIGURE 5: Effect of methanol on mantATP binding. Binding constants were determined from the individual isotherms at each solvent concentration. The change in K_1 and K_2 is shown as a function of solvent present. For each solvent concentration (%), the appropriate enhancement factor was used, as follows: 0%, 2.3; 5%, 2.0; 10%, 2.0; 15%, 1.9; 20%, 1.6. Solid line (—):K_1. Dashed line (---): K_2.

(26), the lifetimes were determined and the fluorescence enhancement factors calculated for each solvent condition used.

Methanol in the concentration range 0−20% (v/v) lowers the binding affinity of mantATP at the first site by up to 55% (Figure 5) while the affinity at the second site falls by 20%. Under similar conditions, the ATPase activity of dynein is stimulated with a more profound ∼2.5-fold irreversible increase at 20% methanol (42, 43). Enhancement factors decreased with increasing methanol (Figure 5, legend).

Similar treatment of dynein with the nonionic detergent, Triton X-100 (poly(ethylene glycol) *tert*-octylphenyl ether), reduced the binding affinity for mantATP by 13% and 20% at 0.1% and 0.2% (v/v) Triton, respectively. Triton X-100 concentrations up to 0.2% did not affect the quantum yield or fluorescence enhancement factor of mantATP upon binding to dynein. Exposing dynein to 0.2% Triton X-100 has been shown to result in an 8−10-fold irreversible increase in its ATPase activity (42, 43).

Effect of Polar Factors. As a complement to the solvent experiments, the effects of various salts on binding affinity were also investigated (Figure 6). If the predominant component of binding of mantATP to dynein were polar, then an increase in ionic strength might be expected to diminish the affinity. Moderate concentrations of NaCl (<0.8 M) increased the binding affinity of mantATP at the K_1 site by ∼60% (Figure 6A), whereas at higher concentrations the affinity decreased. Sodium acetate had a similar but smaller effect on binding, whereas K_2SO_4 gradually decreased the affinity at the first site by ∼40% over the ionic strength range 0−1.33 M. Similar but lesser changes occurred at the K_2 site (Figure 6B). These changes in affinity do not parallel the effect of the salts on dynein ATPase activity, where NaCl shows a reversible 15-fold activation over the same concentration range and sodium acetate shows a much smaller, 2-fold, stimulation (42, 43).
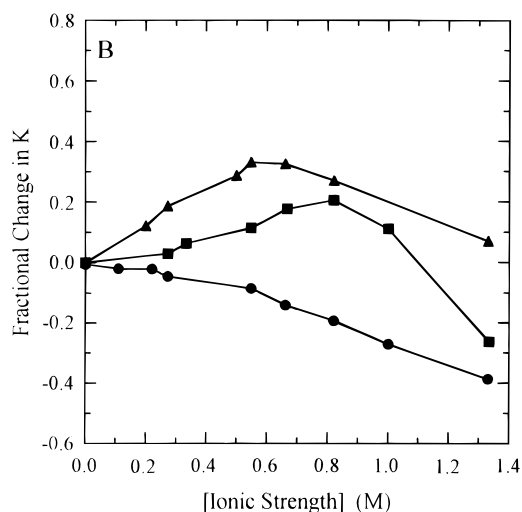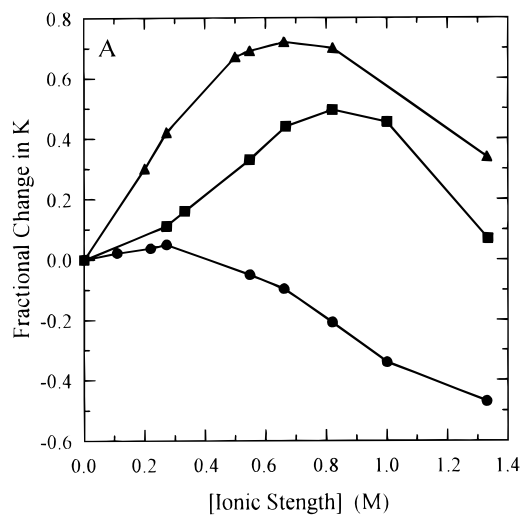

FIGURE 6: Salt dependence of binding constants K_1 and K_2. Titration of mantATP with dynein was carried out in the presence of various concentrations of NaCl (triangle), sodium acetate (square), and K_2SO_4 (circle). Binding constants were determined for each individual isotherm. The changes in K_1 (A) and K_2 (B) are shown as a function of ionic strength of the medium.

DISCUSSION

MantATP is amphiphilic in nature, possessing both polar and apolar moieties, and its fluorescence properties are sensitive to the microenvironment of the binding site on a protein. The increase of fluorescence anisotropy upon binding of mantATP to dynein and its heavy chain subfractions has allowed direct determination of binding affinity by anisotropy titration, as well as study of the changes in affinity resulting from addition of different polar and apolar components to the solvent.

Since mantATP bound to dynein can be displaced by unsubstituted ATP and ADP added to the medium, it is likely that mantATP binds specifically to the same site(s) as the unsubstituted nucleotide. This result is consistent with previous reports that mantATP shows little or no nonspecific binding to other ATPases (ref 28, and references therein).

The 2.2-fold increase in lifetime of mantATP upon binding to dynein is in good agreement with the enhancement factors observed for the binding of other mant-nucleotides to various proteins (28). The ATPase motor protein myosin binds mantATP with an apparently identical enhancement factor

of 2.2 (*27*). The high extrapolated value of the anisotropy suggests that mantATP complexed with dynein experiences substantially restricted mobility during its 8−9 ns lifetime.

The lifetime component due to bound mantATP was homogeneous in standard assay buffer, consistent with data for mantATP bound to other proteins (*27, 28*). Since mantATP is hydrolyzed by dynein, the fluorescence presumably arises from a range of kinetic intermediates. The observed value of the bound lifetime thus represents an average of bound mantATP and its hydrolysis product, mantADP, at different sites and conformations. That is, the homogeneous bound lifetime, within experimental error, is independent of the kinetic intermediate of dynein and the ATP binding site to which it is bound. This observation implies that those aspects of the microenvironment which affect the excited state of mant-fluorophore, are similar in all the important intermediates.

The results of anisotropy titrations are in good agreement with previous studies which demonstrated that dynein heavy chains can interact with nucleotides at greater than one to one molar stoichiometry (*23, 21*). The binding isotherms for mantATP suggest that the α and β heavy chains each possess one site of high affinity and at least one site of lower affinity. Analysis of the titration curves, using a multistep equilibrium model, allowed us to determine the affinities of the first two binding sites. The additional weak sites observed previously could not be studied in this work because of practical limitations of protein concentration. The affinity of the high-affinity site of dynein for mantATP appears to be ∼7−8 times greater than the value obtained previously for unsubstituted ATP binding by phase partition analysis, whereas the affinity of the lower-affinity site is only slightly higher. Tighter binding of mant-nucleotides has been reported previously for other proteins (*26, 28*). In the present case, the greater affinity of mantATP may represent a contribution of apolar interactions of the mant group to the free energy of binding. The 7−8-fold higher affinity corresponds to an increase of 1.4−1.6 kcal to the total free energy of binding, which is comparable to the 0.5−1.8 kcal/mol required for displacing hydrogen bonds in proteins (*44*). However, the greater affinity of mantATP as compared to ATP may also derive partly from an artificially low value for the affinity of unsubstituted ATP obtained in the previous work due to the presence of dextran and poly(ethylene glycol) in the partition solvent (*21*). It is notable that our observed value of 27×10^4 M^{-1} ($K_d = 3.7$ μM) for the affinity of mantATP binding to the high-affinity site of dynein is roughly comparable to the Michaelis constant of ∼30 μM reported by Omoto (*30*) for several motility parameters of flagellar axonemes reactivated with mantATP.

In the presence of the ATPase inhibitor vanadate, mantATP binds with up to 33% greater affinity. Maximal increase is observed with 0.1 mM vanadate, which is approximately the concentration required for maximal inhibition of dynein ATPase activity, possibly because trapping the nucleotide with vanadate causes a conformational change near the ribose binding site of the protein that changes the dielectric constant of the microenvironment around the fluorophore. Thus the change in affinity with added vanadate can be due to most or all of the dynein being in the dead-end kinetic block. As the concentration of vanadate is increased beyond 0.1 mM, the affinity for binding of

mantATP decreases, either because of competition for binding from the increasing concentrations of oligovanadate present, or because of a change in the local structure of the dynein/mantADP/V$_i$ complex relative to that of the corresponding dynein/mantADP/P$_i$ complex.

Our data show that, after taking into account the effects on fluorescence lifetime and quantum yield, the binding affinity of dynein for mantATP is diminished only moderately (<60%) by the presence in the medium of up to 20% methanol or 0.2% Triton X-100, although these agents increase the rate of ATP hydrolysis by dynein as much as 10−20-fold (*42, 43*). A similar contrast is observed in the effect of salts on binding affinity and on the rate of ATP hydrolysis. For example, 0.8 M NaCl induces an approximate 70% *increase* in binding affinity for mantATP, whereas it results in a reversible 15-fold activation of dynein ATPase (*42, 43*). It thus appears that the conformational changes in dynein structure upon exposure to these salts and apolar agents result in only a modest destabilization of mantATP binding to the prehydrolytic kinetic intermediates in the catalytic pathway, relative to their much greater destabilization of the dynein/ADP/P$_i$ complex whose dissociation represents the usual rate-limiting step in the overall hydrolysis reaction. ATP binding to dynein has been shown to lead to significant conformational changes that are not limited to the immediate vicinity of the nucleotide-binding site (*29, 45, 46*).

The measured binding affinities show that the individual α and β heavy chains of dynein each possess a minimum of two chemically distinct nucleotide-binding sites of high and low affinity that are able to bind mantATP simultaneously. The evolutionary conservation of the these sites revealed by sequence studies (*20*) suggests that nucleotide binding at both high- and low-affinity sites plays a critical physiological role. Binding and hydrolysis at the high-affinity site presumably provide the energy for motility, while binding at the low-affinity site(s) may serve to optimize the rate of hydrolysis or to regulate the variable energetic costs of driving the conformational changes necessary for force generation during oscillatory axonemal beating. When comparing in vivo and in vitro conditions, one must take into account that macromolecular crowding effects in vivo can result in large contributions, perhaps as much as 2−3 orders of magnitude, to the effective molecular concentrations that could influence nucleotide binding to dynein (*46*). The in vivo concentration of ATP is already relatively high, nearing 0.5−1.0 mM. Local concentration gradients, especially if amplified by crowding effects, could modulate the extent of nucleotide binding to provide a useful level of regulation.

In closing, the present study further defines the interaction of nucleotides with dynein and provides useful information for further application of fluorescent ATP derivatives to clarify the distinct roles of the several conserved nucleotide-binding sites in the biology of dynein.

REFERENCES

1. Gibbons, I. R. (1963) *Proc. Natl. Acad. Sci. U.S.A. 50*, 1002−1010.

2. Gibbons, I. R. (1981) *J. Cell Biol. 91,* 107s−124s.

3. Gibbons, I. R. (1989) in *Cell Movement: The dynein ATPases* (Warner, F. D., Satir, P., Gibbons, I. R., Eds.) Vol. 1, pp 3−22.

4. Vallee, R. B., Wall, J. S., and Paschal, B. M. (1989) *Trends Neurosci. 12,* 66−70.

5. Schnapp, B. J., and Reese, T. S. (1989) *Proc. Natl. Acad. Sci. U.S.A. 85,* 1009−1113.

6. Eshel, D., Urrestarazu, L. A., Vissers, S., Jaunaux, J. C., van Vliet-Reedijk, J. C., Planta, R. J., and Gibbons, I. R. (1993) *Proc. Natl. Acad. Sci. U.S.A.*, *90,* 11172−11176.

7. Pallini, V., Mencarelli, C., Bracci, L., Contorni, M., Ruggiero, P., Tiezzi, A., and Manetti, R. (1983) *J. Submicrosc. Cytol. 15,* 229−235.

8. Paschal, B. M., Shpetner, H. S., and Vallee, R. B. (1987) *J. Cell Biol. 105,* 1273−1282.

9. Lye, R. J., Porter, M. E., Scholey, J. M., and McIntosh, J. R. (1987) *Cell 51,* 309−318.

10. Neely, M. D., Erickson, H. P., and Boekelheide, K. (1990) *J. Biol. Chem. 265,* 8691−8698.

11. Asai, D. J., and Lee, S. W. (1995) *Mol. Cells, 5,* 299−305.

12. Gibbons, I. R., Gibbons, B. H., Mocz, G., and Asai, D. (1991) *Nature 352,* 640−643.

13. Ogawa, K. (1991) *Nature 352,* 643−645.

14. Wilkerson, C. G., King, S. M., and Witman, G. B. (1994) *J. Cell. Sci. 107,* 497−506.

15. Michell, D. R., and Brown, K. S. (1994) *J. Cell Sci. 107,* 635−644.

16. Koonce, M. P., Grissom, P. H., and McIntosh, J. R. (1992) J. *Cell Biol. 119,* 1597−1604.

17. Mikami, A., Paschal. B. M., Mazumdar, M., and Vallee, R. B. (1993) *Neuron 10,* 787−796.

18. Walker, J. E., Saraste, M., Runswick, M. J., and Gay, N. J. (1982) *EMBO J. 1,* 945−951.

19. Gibbons, I. R., and Mocz, G. (1990) in *Vanadium in Biological Systems* (Chasteen, N. D., Ed.) pp 143−152, Kluwer Academic Publishers, Dordrecht, The Netherlands.

20. Gibbons, B. H., Asai, D. J., Tang, W.-J. Y., Hays, T. S., and Gibbons, I. R. (1994) *Mol. Biol. Cell 5,* 57−70.

21. Mocz, G., and Gibbons, I. R. (1996) *Biochemistry 35,* 9204−9211.

22. Kinoshita, S., Miki-Noumura, T., and Omoto, C. K. (1995) *Cell Motil. Cytoskeleton. 32,* 46−54.

23. Wilkerson, C. G., and Witman, G. B. (1995) *Mol. Biol. Cell, 6,* 33a.

24. Omoto, C. K., Yagi, T., Kurimoto, E., and Kamiya, R. (1996) *Cell Motil. Cytoskeleton 33,* 88−94.

25. Johnson, K. A. (1983) *J. Biol. Chem. 258,* 13825−13832.

26. Hiratsuka, T. (1983) *Biochim. Biophys. Acta 742,* 496−508.

27. Cremo, C. R., Neuron, J. M., and Yount, R. G. (1990) *Biochemistry 29,* 3309−3319.

28. Jameson, D. M., and Eccleston, J. F. (1997) *Methods Enzymol. 278,* 363−390.

29. Inaba, K., Okuno, M., and Mohri, H. (1989) *Arch. Biochem. Biophys. 274,* 209−215.

30. Omoto, K. (1992) *J. Muscle Res. Cell Motil. 13,* 635−639.

31. Lark, E., and Omoto, C. K. (1994) *Cell Motil. Cytoskeleton 27,* 161−168.

32. Bell, C. W., Fraser, C., Sale, W. S., Tang, W.-J. Y., and Gibbons, I. R. (1982) *Methods Cell Biol. 24,* 373−397.

33. Gratton, E., Jameson, D. M., and Hall, R. D. (1984) *Annu. Rev. Biophys. Bioeng. 13,* 105−124.

34. Jameson, D. M., and Hazlett, T. L. (1991) in *Biophysical and Biochemical Aspects of Fluorescence Spectroscopy* (Dewey, T. G., Ed.) pp 105−133, Plenum Press, NY.

35. Jablonski, A. (1960) *Bull. Acad. Pol. Sci., Ser. Sci., Math., Astron. Phys. 8,* 259−264.

36. Weber, G. (1952) *Biochem. J. 51,* 145−155.

37. Wentworth, W. E. (1965) *J. Chem. Educ. 42,* 96−103, 162−167.

38. Dawson, R. M. C., Elliott, D. C., Elliott, W. H., and Jones, K. M. (1986) *Data for biochemical research,* pp 105, Oxford Science Publications, Clarendon Press, Oxford, U.K.

39. Whitaker, J. R., and Granum, P. E. (1980) *Anal. Biochem. 109,* 156−159.

40. LeBel, D., Poirier, G. G., and Beaudoin, A. R. (1978) *Anal. Biochem. 85,* 86−89.

41. Shimizu, T., and Johnson, K. A. (1983) *J. Biol. Chem. 258,* 13833−13840.

42. Evans, J. A., Mocz, G., and Gibbons, I. R. (1986) J. *Biol. Chem. 261,* 14039−14043.

43. Evans, J. A., and Gibbons, I. R. (1986) *J. Biol. Chem. 261,* 14044−14048.

44. Fersht, A. R. (1985) *Enzyme structure and mechanism*, 2nd ed., pp 306−307, Freeman, New York.

45. Goodenogh, U., and Heuser, J. (1985) *J. Cell. Biol. 100,* 2008−2018.

46. Jarvis, T. C., Ring, D. M., Daube, S. S., and von Hippel, P. H. (1990) *J. Biol. Chem. 265,* 15160−15167.